

Band-gap-engineered spin-phonon, and spin-spin interactions with defect centers in diamond coupled to phononic crystals

Peng-Bo Li,¹ Xiao-Xiao Li,^{1,2} and Franco Nori^{3,4}

¹*Shaanxi Province Key Laboratory of Quantum Information and Quantum Optoelectronic Devices, Department of Applied Physics, Xi'an Jiaotong University, Xi'an 710049, China*

²*Department of Physics, University of Oregon, Eugene, Oregon 97403, USA*

³*Theoretical Quantum Physics Laboratory, RIKEN Cluster for Pioneering Research, Wako-shi, Saitama 351-0198, Japan*

⁴*Department of Physics, The University of Michigan, Ann Arbor, Michigan 48109-1040, USA*

We study a spin-phononic system where diamond defect centers are interfaced with a quasi-one-dimensional phononic crystal. We show that, a single defect center, coupled to the phonon modes of a phononic crystal waveguide near the band gap, can seed its own phononic cavity mode with an exponentially decaying envelope around the defect center's position. The spin-induced phononic cavity, with a greatly reduced and tunable mode volume, allows coherent phonon-mediated interactions between distant spins with a highly tunable range, enabling access to a variety of long-range interacting spin models. This work opens prospects for exploring quantum many-body physics and quantum information processing with defect centers and periodic phononic nanostructures.

Introduction.— Electronic spins associated with defect centers in diamond comprise an outstanding platform for both fundamental research and practical applications [1–7]. Prominent defect centers in diamond include silicon-vacancy (SiV) [8–14], nitrogen-vacancy (NV) [15] and germanium vacancy (GeV) [16] color centers, which possess the advantage of long coherence times [17, 18] and perfect compatibility with other solid-state setups [19–24].

For the realization of practical quantum technologies, coherent and controllable interactions between distant solid spins play an essential role. To achieve this goal, schemes for interfacing solid spins via mechanical degrees of freedom have been extensively investigated [25–41], where a conventional acoustic cavity (waveguide) [42–45] or mechanical resonator is often employed to mediate effective spin-spin interactions. Nevertheless, there are two challenges in complete quantum control of both spin and mechanical degrees of freedom [46, 47]. First of all, the phonon-mediated spin-spin interaction is often too weak due to the weak intrinsic strain coupling of spins to vibrational modes [48, 49]. Second and more importantly, complete control on spin-spin interactions still remains a challenge. In particular, the spatial range of phonon-mediated spin-spin interactions cannot be tuned or controlled, and is set solely by the dimension of the setup.

In this work, we propose that by utilizing phononic crystals that interface with defect centers, the problem mentioned above can be overcome. Phononic crystals [50–60] naturally enable interactions with a strength potentially much greater, owing to the much tighter confinement of the mediating phonon. The ability to tailor the modal properties and dispersion relation of a phononic crystal waveguide significantly goes beyond that of a conventional acoustic waveguide or cavity, which offers a greatly expanded toolbox for controlling spin-phonon interactions. Particularly, the band gap of a phononic

crystal provides a tunable interaction range, a feature which is unique to this kind of nanostructures, and makes phononic crystals remarkably different from either acoustic cavities or unstructured waveguides [50–60]. We investigate the band gap engineered spin-phonon, and spin-spin interactions with defect centers in diamond interfaced to a quasi-one-dimensional (1D) phononic crystal. We show that, when the transition frequency of the defect center lies within the band gap, the defect center can seed its own phononic cavity mode with an exponentially decaying envelope around its position. This leads to an enhanced spin-phonon coupling due to the much tighter confinement of the phonon. The band-gap interaction between defect centers and phononic crystal modes can realize coherent spin-spin coupling with a highly tunable spatial range, which is not readily achievable using other interaction mechanisms. This work indicates that hybrid systems [61] composed of defect centers and periodic phononic nanostructures comprise a promising platform for the investigation of quantum many-body physics [62] and quantum information processing.

Model.— We consider the setup shown in Fig. 1, where separated defect centers (SiV, NV, and GeV centers) in diamond are coupled to the phonon modes of a 1D phononic crystal waveguide near a band gap. Without loss of generality, we assume that the defect center is coupled via strain to a continuum of compression modes propagating along the phononic crystal (along the x axis). Local lattice distortions associated with internal compression modes of the phononic crystal affect the defect's electronic structure, which induces a strain coupling between these phonons and the orbital degrees of freedom of the center [11, 39].

The phononic crystal, a quasi-1D periodic structure, has a spatially periodic structure with lattice constant a , a cross section A , and total length $L \gg a, \sqrt{A}$. We assume that the transverse dimensions of the phononic crystal are much smaller than the characteristic phonon

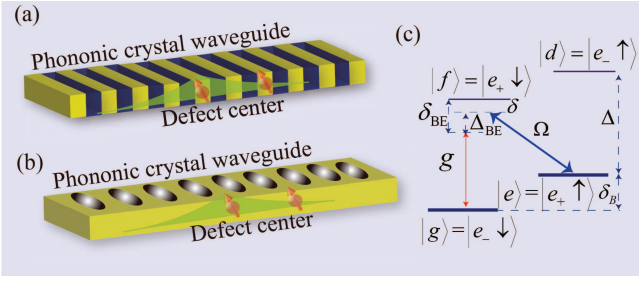


FIG. 1. (Color online) Schematic of two separated defect centers in diamond coupled to the phonon modes of a 1D phononic crystal waveguide near a bandgap. (a) The phononic crystal waveguide is a quasi-1D periodic structure composed of alternating layers of diamond and Si (type I). (b) The phononic crystal waveguide is a 1D phononic crystal consisting of a periodic array of holes in a diamond beam (type II). (c) Driven Λ system of SiV centers, where the transition $|g\rangle \leftrightarrow |f\rangle$ couples with strength g to the phononic crystal modes, while the transition $|e\rangle \leftrightarrow |f\rangle$ is driven by a classical microwave field with detuning δ and Rabi frequency Ω . When $\delta_B \gg \delta$, the state $|d\rangle$ is far off-resonance and can be neglected.

wavelength $\lambda_c = 2\pi v_c/\omega_s$, with v_c the characteristic speed of sound in diamond, and ω_s the effective transition frequency of the defect center. In this case, the transverse modes are far off resonance with the defect center, and only the longitudinal waves are involved in the coupling.

The phononic crystal waveguide supports phonon modes of frequency $\omega_{n,k}$ and mode profile $\vec{Q}_{n,k}(\vec{r})$ [63], where k is the wave vector along the waveguide, and n is the band index. Because of the periodicity of the phononic crystal, the phononic modes are of Bloch form [51]. In the limit of a quasi-1D crystal, $\vec{Q}_{n,k}(\vec{r}) \sim e^{ikx} \vec{u}_{n,k}(\vec{r})$ ($|k| \leq \pi/a$ in the first Brillouin zone). Here $\vec{u}_{n,k}(\vec{r})$ is a periodic function associated with the shape of the Bloch modes, with periodicity given by the lattice constant a . Figure 2 shows finite-element-method (FEM) simulations of the mechanical band structures, and displacement patterns of the symmetric modes at the band edge frequency for the two types of phononic crystal waveguides. The band structure of the phononic crystal waveguide shows a sizable band gap for the mechanical modes, which allows the defect center's transition frequency to lie within the bandgap.

For defect centers such as SiV, NV, and GeV centers, strong coupling between the orbital degrees of freedom and the mechanical vibrations can be obtained through the ground states or excited states [11, 27, 39, 64]. Here we take SiV centers as an example, but the general model also applies to NV and GeV centers. The SiV center is a point defect in which a silicon atom is positioned between two adjacent missing carbon atoms in the diamond lattice [11]. Its electronic ground state is formed by an unpaired hole of spin $S = 1/2$, which occupies one of

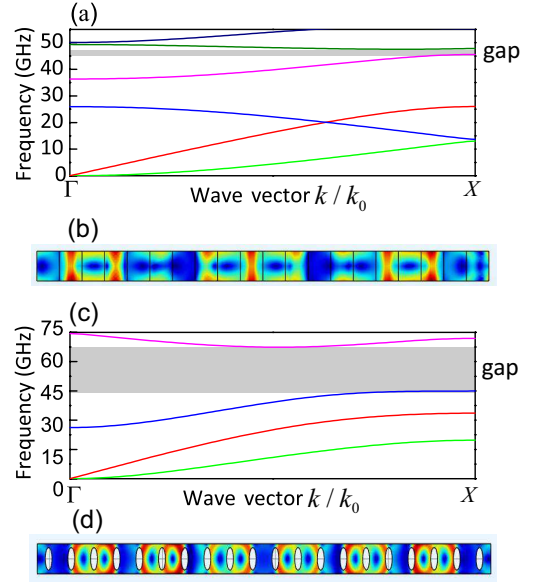


FIG. 2. (Color online) (a) Phononic band structure of the quasi-1D phononic crystal waveguide of type I. The cross section has a dimension $100 \text{ nm} \times 20 \text{ nm}$, and the crystal has a period of 150 nm . (b) Displacement pattern of the symmetric mode at the band edge frequency ω_{BE} for the type I phononic crystal. (c) and (d) show the corresponding results for the type II phononic crystal, which has a width of 100 nm , and a period of 100 nm . For the elliptical holes in the waveguide, the minor (major) axis is 30 nm (76 nm).

the two degenerate orbital states $|e_x\rangle$ and $|e_y\rangle$ [63]. In the presence of spin-orbit interactions and a weak Jahn-Teller effect, the four states are split into two doublets [11], $\{|g\rangle = |e_- \downarrow\rangle, |e\rangle = |e_+ \uparrow\rangle\}$ and $\{|f\rangle = |e_+ \downarrow\rangle, |d\rangle = |e_- \uparrow\rangle\}$. Here, $|e_{\pm}\rangle = (|e_x\rangle \pm i|e_y\rangle)/\sqrt{2}$ are eigenstates of the orbital angular momentum operator \hat{L}_z , with the z axis along the symmetry axis of the defect. The energy gap between these doublets is $\Delta/2\pi = 46 \text{ GHz}$ [11].

The interaction Hamiltonian is given by $H_{\text{strain}} = \sum_{ij} V_{ij} \epsilon_{ij}$ [11, 36, 63], where V_{ij} is an operator acting on the electronic states of the defect center, and ϵ is the strain tensor. The strain Hamiltonian can be projected onto the irreducible representations of the D_{3d} group for SiV centers, which reflects the symmetry of the orbital wavefunctions, i.e., $H_{\text{strain}} = \hbar \sum_l V_l \epsilon_l$. Each ϵ_l is a linear combination of strain components $\epsilon_{i,j}$, and corresponds to specific symmetries indicated by the subscript l , i.e., $\epsilon_{A_{1g}} = t_{\perp}(\epsilon_{xx} + \epsilon_{yy}) + t_{\parallel} \epsilon_{zz}$, $\epsilon_{E_{gx}} = d(\epsilon_{xx} - \epsilon_{yy}) + f \epsilon_{zx}$, and $\epsilon_{E_{gy}} = -2d \epsilon_{xy} + f \epsilon_{zx}$. Here t_{\perp} , t_{\parallel} , d , and f are the four strain-susceptibility parameters that completely describe the strain-response of the orbital states $|e_x\rangle$ and $|e_y\rangle$. The strain Hamiltonian can be rewritten in the basis spanned by the eigenstates of the spin-orbit coupling [30] $H_{\text{strain}} = \hbar \epsilon_{E_{gx}} (L_- + L_+) - i \hbar \epsilon_{E_{gy}} (L_- - L_+)$, where $L_+ = L_-^\dagger = |f\rangle \langle g| + |e\rangle \langle d|$ is the orbital raising operator

within the ground state.

Upon quantization, the mechanical displacement $\vec{Q}(\vec{r})$ becomes an operator, which can be expressed in terms of the elementary normal modes and annihilation operators as $\hat{Q}(\vec{r}) = \sum_{n,k} [\hat{Q}_{n,k}(\vec{r})\hat{a}_{n,k} + \text{H.c.}]$ [63, 65]. The resulting strain coupling can be written in the general form $\hat{H}_{\text{strain}} \simeq \sum_{n,k} [\hbar g_{n,k}\hat{a}_{n,k}\hat{J}_+ e^{ikx} + \text{H.c.}]$ [63], where the coupling constant $g_{n,k}$ depends on the local strain tensor and can be evaluated for a known mode profile $\vec{Q}_{n,k}(\vec{r})$, and $\hat{J}_+ = |f\rangle\langle g| + |d\rangle\langle e|$. The defect center is coupled predominantly to only a single band of the phononic crystal waveguide, via tuning the transition frequency Δ of the color center close to the band edge frequency ω_{BE} , with detuning $\delta_{\text{BE}} = \Delta - \omega_{\text{BE}}$ (where $\delta_{\text{BE}} > 0$, so that the spin frequency lies within the band gap). We assume that the detuning to any other band edge is much larger than δ_{BE} , so the other bands can be neglected. For clarity, we omit the band index n in the following discussion.

Phononic bound state and effective acoustic cavity.— When the transition frequency of the defect center is tuned close to the band edge, the spin is dominantly coupled to the modes near the band edge wavevector $k_0 = \pi/a$ due to the van Hove singularity in the density of states, i.e., $\frac{\partial k}{\partial \omega_k}|_{k_0} \rightarrow \infty$. In this case, the dispersion relation can be approximated to be quadratic $\omega_k \simeq \omega_{\text{BE}} - \alpha a^2(k - k_0)^2$, with α a parameter characterizing the band curvature. In the presence of a static magnetic field $\vec{B} = B_0\vec{e}_z$ and a microwave driving field of frequency ω_0 and Rabi-frequency Ω along \vec{e}_x , we can implement a Raman transition between the states $|g\rangle$ and $|e\rangle$ via the excited state $|f\rangle$ through coupling the SiV center to the mechanical modes. The Hamiltonian of the whole system can be written as [63]

$$\hat{\mathcal{H}} = \sum_k \hbar\omega_k \hat{a}_k^\dagger \hat{a}_k + \hbar\omega_s \hat{\sigma}_{ee} \quad (1)$$

$$+ \sum_k \hbar g_{\text{eff}} (\hat{a}_k^\dagger \hat{\sigma}_{ge} e^{-ikx_0} + \hat{a}_k \hat{\sigma}_{eg} e^{ikx_0}),$$

where $\hat{\sigma}_{ij} = |i\rangle\langle j|$, $\omega_s = \Delta - \delta$, $g_{\text{eff}} = g_k\Omega/\delta$, and g_k is the coupling strength between the defect center (with the position \vec{r}_0) and phonon modes in the band. Moreover, for the modes near the band edge the coupling strength g_k is approximately independent of k , i.e., $g_k \sim g \sim \frac{d}{v_l} \sqrt{\hbar\omega_{\text{BE}}/2\pi\rho aA}$ [63], where $d/2\pi \sim 1$ PHz/strain is the strain sensitivity, and $v_l = 1.71 \times 10^4$ m/s is the speed of sound in diamond.

For a single excitation in the system, there exists a bound state $|\varphi_b\rangle = \cos\theta|0\rangle|e\rangle + \sin\theta|1\rangle|g\rangle$ within the bandgap with the eigenenergy $\hbar\Omega_b$. Here $|0\rangle$ is the vacuum state for the phonon modes, and $|1\rangle = \int dk c_k \hat{a}_k^\dagger |0\rangle$ is a single phonon excitation of the modes in the band. The bound state and the corresponding eigenenergy are determined by the eigenvalue equation $\hat{\mathcal{H}}|\varphi_b\rangle = \hbar\Omega_b|\varphi_b\rangle$.

Solving this equation yields [63]

$$\Omega_b - \omega_s = \frac{\pi g_{\text{eff}}^2}{\sqrt{\alpha(\Omega_b - \omega_{\text{BE}})}}$$

$$\tan^2(\theta) = \frac{\omega_s - \Omega_b}{2(\omega_{\text{BE}} - \Omega_b)}$$

$$c_k = \frac{g_{\text{eff}} e^{-ikx_0}}{\tan\theta(\Omega_b - \omega_k)}. \quad (2)$$

In real space, the phononic part of the bound state is exponentially localized around the spin with spatial mode envelope

$$\mathcal{E}(x) = \int dk c_k Q_k(x) = \sqrt{\frac{2\pi}{L_c}} e^{-|x-x_0|/L_c} Q_{k_0}, \quad (3)$$

where the localization length L_c is given by

$$L_c = a \sqrt{\frac{\alpha}{\Omega_b - \omega_{\text{BE}}}}. \quad (4)$$

This localized phononic cloud has the same properties as a confined acoustic cavity mode. The localization of the phononic wavefunction is determined predominantly by the properties of the band edge, and the frequency detunings, leading to the possibility of dynamic tuning of the localization length.

The coupling between the defect center and the phononic crystal modes near the band edge can be well understood by mapping to the Jaynes-Cummings model in cavity quantum-electrodynamics [66, 67] or spin-mechanics. In particular, the eigenstate $|\varphi_b\rangle$ looks identical in form to one of the dressed eigenstates of the Jaynes-Cummings model. This mapping can be made formal: the phonon confined around the defect center has the same functionality as the mode of an actual acoustic cavity. We can associate an effective spin-phonon coupling strength $g_c = g_{\text{eff}}\sqrt{2\pi a/L_c}$ with the bandgap setup. The effective vacuum-Rabi splitting g_c is identical to that of a real cavity whose mode volume is the same as the bound phonon size $V_{\text{eff}} = AL_c$. This effective spin-phonon interaction can be much stronger than that of defect centers coupling to a conventional phononic waveguide [30], via tuning the effective acoustic cavity mode volume to a much smaller value such that the phonons are confined much tighter. The effective acoustic cavity frequency is the average frequency of the phonon modes, i.e., $\int dk |c_k|^2 \omega_k = \omega_{\text{BE}} - \delta_b$, and the effective spin-cavity detuning is $\Delta_E = \Delta_{\text{BE}} + \delta_b$.

In Fig. 3(a)-(c), we present the numerical simulations for the dependence of the bound-state eigenfrequency Ω_b , the defect center's excited state population $P_e = \cos^2\theta$, and the length of the effective phononic cavity L_c on detuning Δ_{BE} . Fig. 3(a) shows that when $\Delta_{\text{BE}}/g_\alpha \ll -1$, then Ω_b approaches ω_{BE} , while Ω_b approaches $\omega_{\text{BE}} + \Delta_{\text{BE}}$ when $\Delta_{\text{BE}}/g_\alpha \gg 1$. Fig. 3(b) shows that when $\Delta_{\text{BE}}/g_\alpha \ll -1$, the state becomes mostly phononic: a cavity mode dressed by the spin. From Fig. 3(c), one

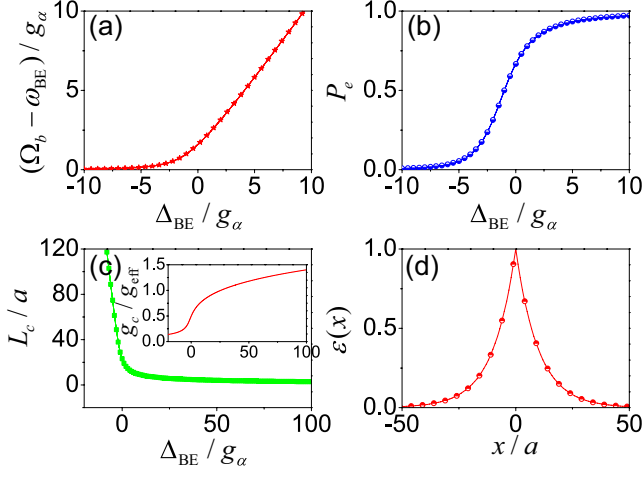


FIG. 3. (Color online) (a) The bound-state eigenfrequency Ω_b relative to the band edge versus detuning $\Delta_{\text{BE}} = \delta_{\text{BE}} - \delta$. (b) The defect center's excited state population $P_e = \cos^2 \theta$ as a function of detuning Δ_{BE} . (c) The length of the effective phononic cavity L_c versus detuning Δ_{BE} . The inset shows the coupling strength versus detuning Δ_{BE} . (d) Spatial profile of the phononic wave function $\mathcal{E}(x)$, for which we choose $L_c = 10a$ and $x_0 = 0$. In the simulations, we choose the parameters for the type I phononic crystal as $\omega_{\text{BE}}/2\pi = 45.5$ GHz, $\alpha/2\pi = 3.5$ GHz, $a = 150$ nm, $A = 100$ nm \times 20 nm, $g_{\text{eff}} = 0.1g$, and $g_\alpha = (\pi g_{\text{eff}}^2 / \sqrt{4\alpha})^{2/3}$.

can see that localized phonon arises with larger detuning Δ_{BE} or flatter bands, giving rise to an enhancement of the effective spin-phonon coupling. From Fig. 3(d), we find that the phononic component of the hybrid spin-phonon state extends over multiple sites.

Spin-spin interactions mediated by phononic crystals.— The band-gap interaction allows us to use the phononic crystal modes as a quantum bus to perform more complex tasks. Analogous to the spin-exchange interaction in cavity QED, two defect centers that are separated by a distance on the order of the length L_c can exchange a phonon excitation via the induced acoustic cavity mode. Based on this effective interaction, it is possible to implement quantum information processing and a variety of interacting spin models [62] with distant defect spins.

We consider two separated SiV centers coupled to the same phononic crystal modes near the band edge, through Raman transitions between the states $|g\rangle$ and $|e\rangle$. In the interaction picture, we can obtain the interaction between the defect centers and phononic crystal modes $\hat{H} = \sum_{j=1,2} \sum_k \hbar g_{\text{eff}}^j (\hat{a}_k^\dagger \hat{\sigma}_{ge}^j e^{-i\delta_k t - ikx_j} + \hat{a}_k \hat{\sigma}_{eg}^j e^{i\delta_k t + ikx_j})$, with $\delta_k = \omega_s - \omega_k$. In the dispersive regime $\delta_k \gg g_{\text{eff}}^j$, this will lead to an effective spin-spin interaction via the exchange of virtual phonons [63],

$$\begin{aligned} \hat{\mathcal{H}}_{s-s} &= \hbar J_{12} \hat{\sigma}_{eg}^1 \hat{\sigma}_{ge}^2 + \text{H.c.} \\ &= \hbar \lambda_{\text{eff}} e^{-|x_1 - x_2|/L_c} \hat{\sigma}_{eg}^1 \hat{\sigma}_{ge}^2 + \text{H.c.}, \end{aligned} \quad (5)$$

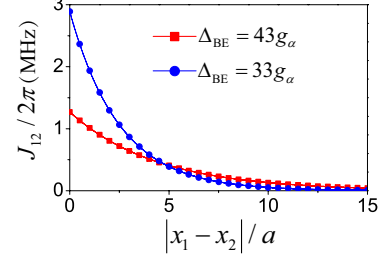


FIG. 4. (Color online) The coupling strength of band gap mediated dipole-dipole interactions J_{12} versus $|x_1 - x_2|$ for different detunings Δ_{BE} . Other parameters are chosen as those in Fig. 3.

with the effective coupling strength $\lambda_{\text{eff}} = g_c^2/2\Delta_{\text{BE}}$. Here the spatial range reflects the shape of the localized phononic cloud.

Different from the dipole-dipole interactions mediated by a conventional cavity, the form of the band-gap-mediated interactions between spins is to decay exponentially with spin separation [68], as shown in Fig. 4. Furthermore, the range of the interaction can be tuned through the effective interaction length L_c , the length scale of which can be on the order of the length of experimental setups, and thus effectively long-range over the system size. Therefore, the band gap interaction can realize coherent spin-spin interactions with a highly tunable range, which cannot be readily achieved using other interaction mechanisms. This potentially enables the study of a variety of interacting spin models [63], and the deterministic generation of entanglement and quantum state transfer between spins at a distance of several lattice constants through a phononic channel.

We assume that the two defect centers are initially prepared in the state $\psi(0) = |g\rangle_1 |e\rangle_2$. Then under the Hamiltonian $\hat{\mathcal{H}}_{s-s}$, the state evolution of the system is given by $\psi(t) = \cos(J_{12}t) |g\rangle_1 |e\rangle_2 - i \sin(J_{12}t) |e\rangle_1 |g\rangle_2$, which is an entangled state for the two centers. If we choose $J_{12}\tau = \pi/4$, we can obtain the maximally entangled two-particle state $\psi(\tau) = \frac{1}{\sqrt{2}} (|g\rangle_1 |e\rangle_2 - i |e\rangle_1 |g\rangle_2)$, which is the well-known Einstein-Podolsky-Rosen state. The interaction (5) between the two defect centers can also be used to transfer arbitrary quantum information encoded in ground spin states from one center to the other: $(\alpha |g\rangle_1 + \beta |e\rangle_1) |e\rangle_2 \rightarrow (\alpha |g\rangle_2 + \beta |e\rangle_2) |e\rangle_1$.

Fig. 5 displays the numerical results for the time evolution of the concurrence and populations for two defect centers under ideal and realistic conditions through solving the master equation using the QuTiP library [69]. We find that, the concurrence and populations are significantly affected by the distance between the centers, even though the other conditions are the same. Moreover, if the decoherence of the defect centers is taken into account, for distances between the centers larger than L_c ,

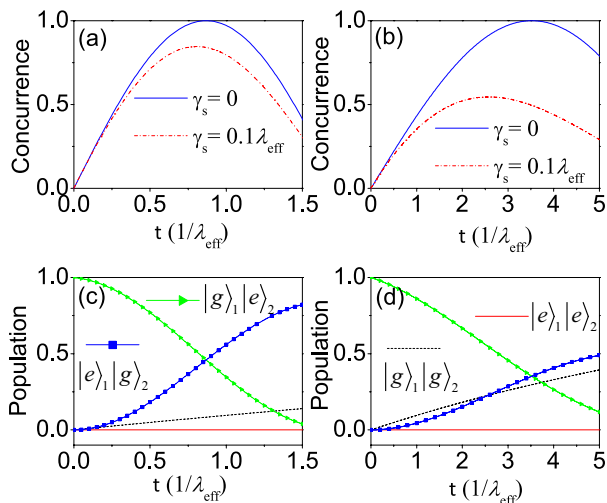


FIG. 5. (Color online) Time evolution of the concurrence and populations. For (a) and (c) the distance between the two defect centers is $|x_1 - x_2| = 0.1L_c$, while for (b) and (d) the distance between them is $|x_1 - x_2| = 1.5L_c$. The results given in (c) and (d) are for $\gamma_s = 0.1\lambda_{\text{eff}}$.

the produced entangled states and the quantum state transfer efficiency will be significantly spoiled.

For the setups illustrated in Fig. 1, the band edge frequency is $\omega_{\text{BE}}/2\pi = 45.5$ GHz, and the quality factor of a phononic crystal mode can reach $Q_m \sim 10^7$, resulting in a mechanical damping rate $\gamma_m/2\pi \sim 5$ kHz. This high mechanical quality factor should be achievable with the use of phononic crystal shields and with the state-of-the-art nanofabrication technologies [56, 70, 71]. At mK temperatures, the thermal phonon number is far below 1 and the spin dephasing rate of SiV centers is about $\gamma_s/2\pi \sim 0.1$ kHz with dynamical decoupling [10]. Even taking into account the surface effect on SiV centers' decoherence, the spin dephasing rate is still expected to be about $\gamma_s/2\pi \sim 100$ kHz. The coupling strength for the design in Fig. 1(a) can be calculated as $g/2\pi \sim 178$ MHz. If we choose $\Omega \sim g$, $\delta \sim 10g$, and $\Delta_{\text{BE}} = 43g_\alpha$, then we have $g_{\text{eff}} \sim 0.1g$, $g_c/2\pi \sim 21.2$ MHz, and $\lambda_{\text{eff}}/2\pi \sim 1.27$ MHz. The time for generating the entangled state and implementing quantum state transfer is about $\tau \leq 1\mu\text{s}$, which is smaller than the coherence time of the setup.

Conclusions. – We have investigated the band gap engineered spin-phonon, and spin-spin interactions with defect centers in diamond coupled to a quasi-1D phononic crystal. We show that, when the transition frequency of the defect center lies within a band gap, the defect center can seed its own phononic cavity mode with an exponentially decaying envelope around its position. The band-gap interaction allows coherent phonon-mediated interactions between spins with a tunable spatial range. The scheme presented in this work is general and can be applied to other defect centers or solid-state systems such

as SiC-based systems [72] and hexagonal boron nitride emitters [73]. This work opens prospects for exploring quantum many-body physics and quantum information processing with defect centers and phononic nanostructures.

X.X.L. acknowledges helpful discussions with Mark C. Kuzyk and Prof. Hailin Wang. P.B.L is supported by the NSFC under Grant Nos. 11774285, 91536115 and 11534008, and the Fundamental Research Funds for the Central Universities. F.N. is supported in part by the: MURI Center for Dynamic Magneto-Optics via the Air Force Office of Scientific Research (AFOSR) (FA9550-14-1-0040), Army Research Office (ARO) (Grant No. Grant No. W911NF-18-1-0358), Asian Office of Aerospace Research and Development (AOARD) (Grant No. FA2386-18-1-4045), Japan Science and Technology Agency (JST) (via the Q-LEAP program, the ImpACT program, and the CREST Grant No. JPMJCR1676), Japan Society for the Promotion of Science (JSPS) (JSPS-RFBR Grant No. 17-52-50023, and JSPS-FWO Grant No. VS.059.18N), the RIKEN-AIST Challenge Research Fund, and the John Templeton Foundation.

-
- [1] I. Buluta, S. Ashhab, and F. Nori, “Natural and artificial atoms for quantum computation,” *Rep. Prog. Phys.* **74**, 104401 (2011).
 - [2] Igor Aharonovich, Andrew D. Greentree, and Steven Prawer, “Diamond photonics,” *Nat. Photon.* **5**, 397 (2011).
 - [3] Igor Aharonovich, Dirk Englund, and Milos Toth, “Solid-state single-photon emitters,” *Nat. Photonics* **10**, 631 (2016).
 - [4] L. Childress, R. Walsworth, and M. D. Lukin, “Atom-like crystal defects,” *Phys. Today* **67**, 38 (2014).
 - [5] G. Balasubramanian, I. Y. Chan, R. Kolesov, M. Al-Hmoud, J. Tisler, C. Shin, C. Kim, A. Wojcik, P. R. Hemmer, A. Krueger, T. Hanke, A. Leitenstorfer, R. Bratschitsch, F. Jelezko, and J. Wrachtrup, “Nanoscale imaging magnetometry with diamond spins under ambient conditions,” *Nature* **455**, 648 (2008).
 - [6] J. R. Maze, P. L. Stanwix, J. S. Hodges, S. Hong, J. M. Taylor, P. Cappellaro, L. Jiang, M. V. Gurudev Dutt, E. Togan, A. S. Zibrov, A. Yacoby, R. L. Walsworth, and M. D. Lukin, “Nanoscale magnetic sensing with an individual electronic spin in diamond,” *Nature* **455**, 644 (2008).
 - [7] C. Zu, W.-B. Wang, L. He, W.-G. Zhang, C.-Y. Dai, F. Wang, and L.-M. Duan, “Experimental realization of universal geometric quantum gates with solid-state spins,” *Nature* **514**, 72 (2014).
 - [8] C. Hepp, T. Müller, V. Waselowski, J. N. Becker, B. Pingault, H. Sternschulte, D. Steinmüller-Nethl, A. Gali, J. R. Maze, M. Atatüre, and C. Becher, “Electronic structure of the silicon vacancy color center in diamond,” *Phys. Rev. Lett.* **112**, 036405 (2014).
 - [9] A. Sipahigil, K. D. Jahnke, L. J. Rogers, T. Teraji,

- J. Isoya, A. S. Zibrov, F. Jelezko, and M. D. Lukin, “Indistinguishable photons from separated silicon-vacancy centers in diamond,” *Phys. Rev. Lett.* **113**, 113602 (2014).
- [10] D. D. Sukachev, A. Sipahigil, C. T. Nguyen, M. K. Bhaskar, R. E. Evans, F. Jelezko, and M. D. Lukin, “Silicon-vacancy spin qubit in diamond: A quantum memory exceeding 10 ms with single-shot state readout,” *Phys. Rev. Lett.* **119**, 223602 (2017).
- [11] Srujan Meesala, Young-Ik Sohn, Benjamin Pingault, Linbo Shao, Haig A. Atikian, Jeffrey Holzgrafe, Mustafa Gündoğan, Camille Stavrakas, Alp Sipahigil, Cleaven Chia, Ruffin Evans, Michael J. Burek, Mian Zhang, Lue Wu, Jose L. Pacheco, John Abraham, Edward Bielejec, Mikhail D. Lukin, Mete Atatüre, and Marko Lončar, “Strain engineering of the silicon-vacancy center in diamond,” *Phys. Rev. B* **97**, 205444 (2018).
- [12] L. J. Rogers, M. H. Metsch K. D. Jahnke and, A. Sipahigil, J. M. Binder, T. Teraji, H. Sumiya, J. Isoya, M. D. Lukin, P. Hemmer, and F. Jelezko, “All-optical initialization, readout, and coherent preparation of single silicon-vacancy spins in diamond,” *Phys. Rev. Lett.* **113**, 263602 (2014).
- [13] J. N. Becker, J. Görlitz, C. Arend, M. Markham, and C. Becher, “Ultrafast all-optical coherent control of single silicon vacancy colour centres in diamond,” *Nat. Commun.* **7**, 13512 (2016).
- [14] Y. Zhou, A. Rasmita, K. Li, Q. Xiong, I. Aharonovich, and W.-B. Gao, “Coherent control of a strongly driven silicon vacancy optical transition in diamond,” *Nat. Commun.* **8**, 14451 (2017).
- [15] M. W. Doherty, N. B. Manson, P. Delaney, F. Jelezko, J. Wrachtrup, and Lloyd C. L. Hollenberg, “The nitrogen-vacancy colour centre in diamond,” *Phys. Rep.* **528**, 1 (2013).
- [16] M. K. Bhaskar, D. D. Sukachev, A. Sipahigil, R. E. Evans, M. J. Burek, C. T. Nguyen, L. J. Rogers, P. Siyushev, M. H. Metsch, H. Park, F. Jelezko, M. Loncar, and M. D. Lukin, “Quantum nonlinear optics with a germanium-vacancy color center in a nanoscale diamond waveguide,” *Phys. Rev. Lett.* **118**, 223603 (2017).
- [17] G. Balasubramanian, P. Neumann, D. Twitchen, M. Markham, R. Kolesov, N. Mizuochi, J. Isoya, J. Achard, J. Beck, J. Tissler, V. Jacques, P. R. Hemmer, F. Jelezko, and J. Wrachtrup, “Ultralong spin coherence time in isotopically engineered diamond,” *Nature Mater.* **8**, 383 (2009).
- [18] N. Bar-Gill, L. M. Pham, A. Jarmola, D. Budker, and R. L. Walsworth, “Solid-state electronic spin coherence time approaching one second,” *Nat. Commun.* **4**, 1743 (2013).
- [19] David D. Awschalom, Lee C. Bassett, Andrew S. Dzurak, Evelyn L. Hu, and Jason R. Petta, “Quantum spintronics: Engineering and manipulating atom-like spins in semiconductors,” *Science* **339**, 1174 (2013).
- [20] A. Sipahigil, R. E. Evans, D. D. Sukachev, M. J. Burek, J. Borregaard, M. K. Bhaskar, C. T. Nguyen, J. L. Pacheco, H. A. Atikian, C. Meuwly, R. M. Camacho, F. Jelezko, E. Bielejec, H. Park, M. Lončar, and M. D. Lukin, “An integrated diamond nanophotonics platform for quantum-optical networks,” *Science* **354**, 847 (2016).
- [21] D. Marcos, M. Wubs, J. M. Taylor, R. Aguado, M. D. Lukin, and A. S. Sørensen, “Coupling nitrogen-vacancy centers in diamond to superconducting flux qubits,” *Phys. Rev. Lett.* **105**, 210501 (2010).
- [22] Xiaobo Zhu, Shiro Saito, Alexander Kemp, Kosuke Kakuyanagi, Shin ichi Karimoto, Hayato Nakano, William J. Munro, Yasuhiro Tokura, Mark S. Everitt, Kae Nemoto, Makoto Kasu, Norikazu Mizuochi, and Kouichi Semba, “Coherent coupling of a superconducting flux qubit to an electron spin ensemble in diamond,” *Nature* **478**, 221 (2011).
- [23] Peng-Bo Li, Yong-Chun Liu, S.-Y. Gao, Ze-Liang Xiang, Peter Rabl, Yun-Feng Xiao, and Fu-Li Li, “Hybrid quantum device based on NV centers in diamond nanomechanical resonators plus superconducting waveguide cavities,” *Phys. Rev. Applied* **4**, 044003 (2015).
- [24] Peng-Bo Li and Franco Nori, “Hybrid quantum system with nitrogen-vacancy centers in diamond coupled to surface-phonon polaritons in piezomagnetic superlattices,” *Phys. Rev. Applied* **10**, 024011 (2018).
- [25] Shimon Kolkowitz, Ania C. Bleszynski Jayich, Quirin P. Unterreithmeier, Steven D. Bennett, Peter Rabl, J. G. E. Harris, and Mikhail D. Lukin, “Coherent sensing of a mechanical resonator with a single-spin qubit,” *Science* **335**, 1603 (2012).
- [26] M. J. A. Schuetz, E. M. Kessler, G. Giedke, L. M. K. Vandersypen, M. D. Lukin, and J. I. Cirac, “Universal quantum transducers based on surface acoustic waves,” *Phys. Rev. X* **5**, 031031 (2015).
- [27] D. Andrew Golter, Thein Oo, Mayra Amezcua, Ignas Lekavicius, Kevin A. Stewart, and Hailin Wang, “Coupling a surface acoustic wave to an electron spin in diamond via a dark state,” *Phys. Rev. X* **6**, 041060 (2016).
- [28] D. Andrew Golter, Thein Oo, Mayra Amezcua, Kevin A. Stewart, and Hailin Wang, “Optomechanical quantum control of a nitrogen-vacancy center in diamond,” *Phys. Rev. Lett.* **116**, 143602 (2016).
- [29] Mark C. Kuzyk and Hailin Wang, “Scaling phononic quantum networks of solid-state spins with closed mechanical subsystems,” *Phys. Rev. X* **8**, 041027 (2018).
- [30] M.-A. Lemonde, S. Meesala, A. Sipahigil, M. J. A. Schuetz, M. D. Lukin, M. Loncar, and P. Rabl, “Phonon networks with silicon-vacancy centers in diamond waveguides,” *Phys. Rev. Lett.* **120**, 213603 (2018).
- [31] Peng-Bo Li, Ze-Liang Xiang, Peter Rabl, and Franco Nori, “Hybrid quantum device with nitrogen-vacancy centers in diamond coupled to carbon nanotubes,” *Phys. Rev. Lett.* **117**, 015502 (2016).
- [32] Carlos Sánchez Muñoz, Antonio Lara, Jorge Puebla, and Franco Nori, “Hybrid systems for the generation of nonclassical mechanical states via quadratic interactions,” *Phys. Rev. Lett.* **121**, 123604 (2018).
- [33] S. D. Bennett, N.Y. Yao, J. Otterbach, P. Zoller, P. Rabl, and M. D. Lukin, “Phonon-induced spin-spin interactions in diamond nanostructures: Application to spin squeezing,” *Phys. Rev. Lett.* **110**, 156402 (2013).
- [34] P. Rabl, S. J. Kolkowitz, F. H. L. Koppens, J. G. E. Harris, P. Zoller, and M. D. Lukin, “A quantum spin transducer based on nanoelectromechanical resonator arrays,” *Nat. Phys.* **6**, 602 (2010).
- [35] O. Arcizet, V. Jacques, A. Siria, P. Poncharal, P. Vincent, and S. Seidelin, “A single nitrogen-vacancy defect coupled to a nanomechanical oscillator,” *Nat. Phys.* **7**, 879 (2011).
- [36] D. Lee, K.W. Lee, J. V. Cady, P. Ouartchaiyapong, and A. C. Bleszynski Jayich, “Topical review: Spins and mechanics in diamond,” *J. Opt.* **19**, 033001 (2017).
- [37] S. Hong, M. S. Grinolds, P. Maletinsky, R. L. Walsworth, M. D. Lukin, and A. Yacoby, “Coherent, mechanical

- control of a single electronic spin,” *Nano Lett.* **12**, 3920 (2012).
- [38] P. Rabl, P. Cappellaro, M. V. Gurudev Dutt, L. Jiang, J. R. Maze, and M. D. Lukin, “Strong magnetic coupling between an electronic spin qubit and a mechanical resonator,” *Phys. Rev. B* **79**, 041302(R) (2009).
- [39] K. V. Keesidis, M.-A. Lemonde, A. Norambuena, J. R. Maze, and P. Rabl, “Cooling phonons with phonons: Acoustic reservoir engineering with silicon-vacancy centers in diamond,” *Phys. Rev. B* **94**, 214115 (2016).
- [40] E. R. MacQuarrie, T. A. Gosavi, N. R. Jungwirth, S. A. Bhave, and G. D. Fuchs, “Mechanical spin control of nitrogen-vacancy centers in diamond,” *Phys. Rev. Lett.* **111**, 227602 (2013).
- [41] Young-Ik Sohn, Srujan Meesala, Benjamin Pingault, Haig A. Atikian, Jeffrey Holzgrafe, Mustafa Gündoğan, Camille Stavrakas, Megan J. Stanley, Alp Sipahigil, Joonhee Choi, Mian Zhang, Jose L. Pacheco, John Abraham, Edward Bielejec, Mikhail D. Lukin, Mete Atatüre, and Marko Lončar, “Controlling the coherence of a diamond spin qubit through its strain environment,” *Nat. Commun.* **9**, 2012 (2018).
- [42] Martin V. Gustafsson, Thomas Aref, Anton Frisk Kockum, Maria K. Ekström, Göran Johansson, and Per Delsing, “Propagating phonons coupled to an artificial atom,” *Science* **346**, 207 (2014).
- [43] R. Manenti, A. F. Kockum, A. Patterson, T. Behrle, J. Rahamim, G. Tancredi, F. Nori, and P. J. Leek, “Circuit quantum acoustodynamics with surface acoustic waves,” *Nat. Commun.* **8**, 975 (2017).
- [44] Nils T. Otterstrom, Ryan O. Behunin, Eric A. Kittlaus, and Peter T. Rakich, “Optomechanical cooling in a continuous system,” *Phys. Rev. X* **8**, 041034 (2018).
- [45] M. J. Burek, N. P. de Leon, B. J. Shields, B. J. M. Hausmann, Y. Chu, Q. Quan, A. S. Zibrov, H. Park, M. D. Lukin, and M. Loncar, “Free-standing mechanical and photonic nanostructures in single-crystal diamond,” *Nano Lett.* **12**, 6084 (2012).
- [46] Miles Blencowe, “Quantum electromechanical systems,” *Phys. Rep.* **395**, 159 (2011).
- [47] M. Poot and H. S. J. van der Zant, “Mechanical systems in the quantum regime,” *Phys. Rep.* **511**, 273 (2012).
- [48] J. Teissier, A. Barfuss, P. Appel, E. Neu, and P. Maletinsky, “Strain coupling of a nitrogen-vacancy center spin to a diamond mechanical oscillator,” *Phys. Rev. Lett.* **113**, 020503 (2014).
- [49] Preeti Ovartchaiyapong, Kenneth W. Lee, Bryan A. Myers, and Ania C. Bleszynski Jayich, “Dynamic strain-mediated coupling of a single diamond spin to a mechanical resonator,” *Nat. Commun.* **5**, 4429 (2014).
- [50] Abdelkrim Khelif and Ali Adibi, *Phononic Crystals* (Springer-Verlag New York, 2016).
- [51] M. S. Kushwaha, P. Halevi, L. Dobrzynski, and B. Djafari-Rouhani, “Acoustic band structure of periodic elastic composites,” *Phys. Rev. Lett.* **71**, 2022 (1993).
- [52] Matt Eichenfield, Jasper Chan, Ryan M. Camacho, Kerry J. Vahala, and Oskar Painter, “Optomechanical crystals,” *Nature (London)* **462**, 78 (2009).
- [53] Martin Maldovan, “Sound and heat revolutions in phononics,” *Nature (London)* **503**, 209 (2013).
- [54] Rishi N. Patel, Zhaoyou Wang, Wentao Jiang, Christopher J. Sarabalis, Jeff T. Hill, and Amir H. Safavi-Naeini, “Single-mode phononic wire,” *Phys. Rev. Lett.* **121**, 040501 (2018).
- [55] Amir H. Safavi-Naeini, Jeff T. Hill, Seán Meenehan, Jasper Chan, Simon Gröblacher, and Oskar Painter, “Two-dimensional phononic-photonic band gap optomechanical crystal cavity,” *Phys. Rev. Lett.* **112**, 153603 (2014).
- [56] Behzad Khanaliloo, Harishankar Jayakumar, Aaron C. Hryciw, David P. Lake, Hamidreza Kaviani, and Paul E. Barclay, “Single-crystal diamond nanobeam waveguide optomechanics,” *Phys. Rev. X* **5**, 041051 (2015).
- [57] Yifan Wang, Behrooz Yousefzadeh, Hui Chen, Hussein Nassar, Guoliang Huang, and Chiara Daraio, “Observation of nonreciprocal wave propagation in a dynamic phononic lattice,” *Phys. Rev. Lett.* **121**, 194301 (2018).
- [58] A. H. Safavi-Naeini and O. Painter, “Design of optomechanical cavities and waveguides on a simultaneous bandgap phononic-photonic crystal slab,” *Opt. Express* **18**, 14926 (2010).
- [59] M. J. Burek, J. D. Cohen, S. M. Meenehan, N. El-Sawah, C. Chia, T. Ruelle, S. Meesala, J. Rochman, H. A. Atikian, M. Markham, D. J. Twitchen, M. D. Lukin, O. Painter, and M. Loncar, “Diamond optomechanical crystals,” *Optica* **3**, 1404 (2016).
- [60] Zian Jia, Yanyu Chen, Haoxiang Yang, and Lifeng Wang, “Designing phononic crystals with wide and robust band gaps,” *Phys. Rev. Applied* **9**, 044021 (2018).
- [61] Ze-Liang Xiang, Sahel Ashhab, J. Q. You, and Franco Nori, “Hybrid quantum circuits: Superconducting circuits interacting with other quantum systems,” *Rev. Mod. Phys.* **85**, 623 (2013).
- [62] Franco Nori, R. Merlin, Stephan Haas, Anders W. Sandvik, and Elbio Dagotto, “Magnetic raman scattering in two-dimensional spin-1/2 heisenberg antiferromagnets: Spectral shape anomaly and magnetostrictive effects,” *Phys. Rev. Lett.* **75**, 553 (1995).
- [63] See Supplemental Material for more details.
- [64] K.W. Lee, D. Lee, P. Ovartchaiyapong, J. R. Maze, J. Minguzzi, and A. C. B. Jayich, “Strain coupling of a mechanical resonator to a single quantum emitter in diamond,” *Phys. Rev. Applied* **6**, 034005 (2016).
- [65] M. Aspelmeyer, T. J. Kippenberg, and F. Marquardt, *Cavity Optomechanics* (Springer, Berlin, 2014).
- [66] Sajeev John and Jian Wang, “Quantum electrodynamics near a photonic band gap: Photon bound states and dressed atoms,” *Phys. Rev. Lett.* **64**, 2418 (1990).
- [67] D. E. Chang, J. S. Douglas, A. González-Tudela, C.-L. Hung, and H. J. Kimble, “Colloquium: Quantum matter built from nanoscopic lattices of atoms and photons,” *Rev. Mod. Phys.* **90**, 031002 (2018).
- [68] Ephraim Shahmoon and Gershon Kurizki, “Nonradiative interaction and entanglement between distant atoms,” *Phys. Rev. A* **87**, 033831 (2013).
- [69] J. Johansson, P. Nation, and F. Nori, “Qutip 2: A python framework for the dynamics of open quantum systems,” *Comput. Phys. Commun.* **184**, 1234 (2013).
- [70] Patricio Arrangoiz-Arriola, E. Alex Wollack, Marek Pechal, Jeremy D. Witmer, Jeff T. Hill, and Amir H. Safavi-Naeini, “Coupling a superconducting quantum circuit to a phononic crystal defect cavity,” *Phys. Rev. X* **8**, 031007 (2018).
- [71] G. MacCabe, H. Ren, J. Luo, J. Cohen, H. Zhou, A. Ardizzi, and O. Painter, “Optomechanical measurements of ultra-long-lived microwave phonon modes in a phononic bandgap cavity,” *Bulletin of the American Physical Society* (2018),

- <https://meetings.aps.org/Meeting/MAR18/Session/B27.7>.
- [72] W. F. Koehl, B. B. Buckley, F. J. Heremans, G. Calusine, and D. D. Awschalom, “Room temperature coherent control of defect spin qubits in silicon carbide,” *Nature* (London) **479**, 84 (2011).
- [73] T. T. Tran, K. Bray, M. J. Ford, M. Toth, and I. Aharonovich, “Quantum emission from hexagonal boron nitride monolayers,” *Nat. Nanotechnol* **11**, 37 (2016).

SUPPLEMENTAL MATERIAL:

Phononic crystals

Calculation of mechanical compression modes in diamond phononic crystals

In the main text, we study a quasi-1D periodic structure with lattice constant a , a cross section A , and total length $L \gg a, \sqrt{A}$. With the framework of elastic mechanical theory, mechanical modes can be treated as a continuum field with time-dependent displacement at the position \vec{r} , given by $\vec{Q}(\vec{r}, t)$. The field $\vec{Q}(\vec{r}, t)$ obeys the equation of motion [S1]

$$\rho \frac{\partial^2}{\partial t^2} \vec{Q}(\vec{r}, t) = (\lambda + \mu) \nabla (\nabla \cdot \vec{Q}(\vec{r}, t)) + \mu \nabla^2 \vec{Q}(\vec{r}, t). \quad (\text{S1})$$

Here ρ is the mass density, and λ and μ are the Lamé constants. Waves in periodic structures are best understood in terms of band theory. From Bloch's theorem, we have that in a structure with periodic variation, the time-harmonic solutions to the mechanical wave equations can be expressed as a product of a plane-wave solution e^{ikx} and a periodic function $\vec{u}_{n,k}(\vec{r})$, i.e., $\vec{Q}_{n,k}(\vec{r}) = e^{ikx} \vec{u}_{n,k}(\vec{r})$, with the eigenfrequencies $\omega_{n,k}$. The Lamé constants can be expressed in terms of the Young's modulus E and the Poisson ratio ν

$$\lambda = \frac{\nu E}{(1 + \nu)(1 - 2\nu)}, \quad \mu = \frac{E}{2(1 + \nu)}. \quad (\text{S2})$$

The frequencies $\omega_{n,k}$ and field patterns of the normal modes can be determined by solving the corresponding eigenvalue equations using finite element simulations [S2]. The material properties of diamond we used are $E = 1050$ GPa, $\nu = 0.2$, and $\rho = 3539$ kg/m³, while for silicon the material properties are $E = 170$ GPa, $\nu = 0.28$, and $\rho = 2329$ kg/m³. All modes considered in this work have even mirror symmetry under reflection R_z about the plane perpendicular to the axis z .

Quantization of the displacement fields in diamond phononic crystals

The motion can be quantized following an approach similar to that used for the electromagnetic field in quantum optics [S3]. We define phonon creation and annihilation operators $\hat{a}_{n,k}^\dagger$ and $\hat{a}_{n,k}$ respectively, for each modal solution $\vec{Q}_{n,k}(\vec{r})$ of the equations of elasticity in the structure. Then the field operator can be expressed as

$$\hat{Q}(\vec{r}) = \sum_{n,k} [\vec{Q}_{n,k}(\vec{r}) \hat{a}_{n,k} + \text{H.c.}]. \quad (\text{S3})$$

To calculate the proper normalization of the field profiles, we assume a single-phonon Fock state $|\Psi\rangle = \hat{a}_{n,k}^\dagger |0\rangle$ and calculate the expectation value of additional field energy above vacuum. We find

$$\begin{aligned} E_{\text{mech}} &= 2\omega_{n,k}^2 \int d\vec{r} \rho(\vec{r}) \vec{Q}_{n,k}^*(\vec{r}) \cdot \vec{Q}_{n,k}(\vec{r}) \\ &= 2\rho V_{\text{eff}} \omega_{n,k}^2 \max[|\vec{Q}_{n,k}|^2], \end{aligned} \quad (\text{S4})$$

where the last equality defines the effective mode volume for mode $\{n, k\}$. Setting $Q_0 = \max[|\vec{Q}_{n,k}|]$ and assuming the phonon energy as $E_{\text{mech}} = \hbar\omega_{n,k}$, we arrive at the general result for a phonon mode, $Q_0 = \sqrt{\hbar/2\rho V_{\text{eff}}\omega_{n,k}}$.

SiV centers

As discussed in the main text, the SiV center is a point defect in which a silicon atom is positioned between two adjacent missing carbon atoms in the diamond lattice. Its electronic ground state is formed by an unpaired hole of spin $S = 1/2$, which occupies one of the two degenerate orbital states $|e_x\rangle$ and $|e_y\rangle$. The spin and orbital degeneracy is lifted by the spin-orbit coupling and by the Jahn-Teller effect. In the presence of an external magnetic field \vec{B} , the Hamiltonian for the electronic ground state of the SiV center is [S4]

$$\hat{H}_{\text{SiV}} = -\hbar\lambda_{\text{SO}} \hat{L}_z \hat{S}_z + \hat{H}_{\text{JT}} + \hbar\Upsilon_L B_z \hat{L}_z + \hbar\Upsilon_s \vec{B} \cdot \vec{S}, \quad (\text{S5})$$

where \hat{L}_z and \hat{S}_z are the projections of the angular momentum and spin operators onto the symmetry axis of the defect center (along z axis). λ_{SO} is the spin-orbit coupling strength while Υ_L and Υ_s are the orbital and spin gyromagnetic ratios respectively. In the basis defined by the degenerate eigenstates $\{|e_x \uparrow\rangle, |e_x \downarrow\rangle, |e_y \uparrow\rangle, |e_y \downarrow\rangle\}$, the different contributions to the SiV energy levels, introduced in Eq. (S5), read

$$(\Upsilon_s B_0 - \lambda_{\text{SO}} \hat{L}_z) \hat{S}_z = \frac{1}{2} \begin{bmatrix} \Upsilon_s B_0 & i\lambda_{\text{SO}} \\ -i\lambda_{\text{SO}} & \Upsilon_s B_0 \end{bmatrix} \otimes \begin{bmatrix} 1 & 0 \\ 0 & -1 \end{bmatrix} \quad (\text{S6})$$

$$\hat{H}_{\text{JT}} = \hbar \begin{bmatrix} \mathcal{K}_x & \mathcal{K}_y \\ \mathcal{K}_y & -\mathcal{K}_x \end{bmatrix} \otimes \begin{bmatrix} 1 & 0 \\ 0 & 1 \end{bmatrix}. \quad (\text{S7})$$

In the above equation \mathcal{K}_i represents an energy shift due to local strain in the crystal along axis i . Diagonalizing Eq. (S5) leads to the eigenstates

$$|g\rangle = (\cos \theta |e_x\rangle - ie^{-i\phi} \sin \theta |e_y\rangle) | \downarrow \rangle \quad (\text{S8})$$

$$|e\rangle = (\cos \theta |e_x\rangle + ie^{i\phi} \sin \theta |e_y\rangle) | \uparrow \rangle \quad (\text{S9})$$

$$|f\rangle = (\sin \theta |e_x\rangle + ie^{-i\phi} \cos \theta |e_y\rangle) | \downarrow \rangle \quad (\text{S10})$$

$$|d\rangle = (\sin \theta |e_x\rangle - ie^{i\phi} \cos \theta |e_y\rangle) | \uparrow \rangle, \quad (\text{S11})$$

with

$$\tan \theta = \frac{2\mathcal{K}_x + \Delta}{\sqrt{\lambda_{\text{SO}}^2 + 4\mathcal{K}_y^2}}, \quad \tan \phi = \frac{2\mathcal{K}_y}{\lambda_{\text{SO}}}. \quad (\text{S12})$$

The corresponding eigenenergies are

$$E_{f,g} = (-\Upsilon_s B_0 \pm \Delta)/2, \quad E_{d,e} = (\Upsilon_s B_0 \pm \Delta)/2 \quad (\text{S13})$$

with $\Delta \simeq 2\pi \times 46$ GHz. In this work, we can neglect the small distortions of the orbital states by the JT effect and in the remainder of this work, use the approximation $|g\rangle \simeq |e_- \downarrow\rangle, |e\rangle \simeq |e_+ \uparrow\rangle, |f\rangle \simeq |e_+ \downarrow\rangle, |d\rangle \simeq |e_- \uparrow\rangle$.

Strain coupling of SiV centers to phononic crystal modes

As discussed in the main text, local lattice distortions associated with internal compression modes of the phononic crystal affect the defect's electronic structure, which induces a strain coupling between these phonons and the orbital degrees of freedom of the center. The interaction Hamiltonian is given by

$$H_{\text{strain}} = \sum_{ij} V_{ij} \epsilon_{ij} \quad (\text{S14})$$

where V_{ij} is an operator acting on the electronic states of the defect center, and ϵ is the strain tensor defined by

$$\epsilon_{ij} = \frac{1}{2} \left(\frac{\partial Q_i}{\partial x_j} + \frac{\partial Q_j}{\partial x_i} \right). \quad (\text{S15})$$

In this work we assume that the symmetry axis of the defect center is along the z direction while the phononic crystal is along the x axis. The strain Hamiltonian can be projected onto the irreducible representations of the D_{3d} group for SiV centers, which reflects the symmetry of the orbital wavefunctions, i.e.,

$$H_{\text{strain}} = \hbar \sum_l V_l \epsilon_l. \quad (\text{S16})$$

Each ϵ_l is a linear combination of strain components $\epsilon_{i,j}$, and corresponds to specific symmetries indicated by the subscript l , i.e.,

$$\begin{aligned} \epsilon_{A_{1g}} &= t_{\perp}(\epsilon_{xx} + \epsilon_{yy}) + t_{\parallel} \epsilon_{zz} \\ \epsilon_{E_{gx}} &= d(\epsilon_{xx} - \epsilon_{yy}) + f \epsilon_{zx} \\ \epsilon_{E_{gy}} &= -2d \epsilon_{xy} + f \epsilon_{yz}. \end{aligned} \quad (\text{S17})$$

Here $t_\perp, t_\parallel, d,$ and f are the four strain-susceptibility parameters that completely describe the strain-response of the orbital states $|e_x\rangle$ and $|e_y\rangle$. The effects of these strain components on the electronic states are described by

$$V_{A_{1g}} = |e_x\rangle\langle e_x| + |e_y\rangle\langle e_y| \quad (\text{S18})$$

$$V_{E_{gx}} = |e_x\rangle\langle e_x| - |e_y\rangle\langle e_y| \quad (\text{S19})$$

$$V_{E_{gy}} = |e_x\rangle\langle e_y| + |e_y\rangle\langle e_x| \quad (\text{S20})$$

The strain Hamiltonian can be rewritten in the basis spanned by the eigenstates of the spin-orbit coupling

$$H_{\text{strain}} = \hbar\epsilon_{E_{gx}}(L_- + L_+) - i\hbar\epsilon_{E_{gy}}(L_- - L_+) \quad (\text{S21})$$

where $L_+ = L_-^\dagger = |f\rangle\langle g| + |e\rangle\langle d|$ is the orbital raising operator within the ground state. Upon quantization, the mechanical displacement $\vec{Q}(\vec{r})$ becomes an operator, which can be expressed in terms of the elementary normal modes and annihilation operators as

$$\hat{Q}(\vec{r}) = \sum_{n,k} [Q_0 e^{ikx} \vec{u}_{n,k}(\vec{r}) \hat{a}_{n,k} + \text{H.c.}] \quad (\text{S22})$$

The resulting strain coupling can be written as

$$\hat{H}_{\text{strain}} \simeq \sum_{n,k} [\hbar g_{n,k} \hat{a}_{n,k} \hat{J}_+ e^{ikx_0} + \text{H.c.}] \quad (\text{S23})$$

with the spin-phonon coupling strength given by

$$g_{n,k} = \frac{d}{v_l} \sqrt{\frac{\hbar\omega_{\text{BE}}}{2\pi\rho a A}} \varsigma_{n,k}(\vec{r}). \quad (\text{S24})$$

Here the dimensionless profile is given by

$$\begin{aligned} \varsigma_{n,k}(\vec{r}) = \frac{1}{k} & [(iku_{n,k}^x + \partial_x u_{n,k}^x - \partial_y u_{n,k}^y + \frac{f}{2d} iku_{n,k}^z + \frac{f}{2d} \partial_x u_{n,k}^z + \frac{f}{2d} \partial_y u_{n,k}^x) \\ & - i(-iku_{n,k}^y - \partial_x u_{n,k}^y - \partial_y u_{n,k}^x + \frac{f}{2d} \partial_y u_{n,k}^z + \frac{f}{2d} \partial_z u_{n,k}^y)]. \end{aligned} \quad (\text{S25})$$

For compression modes along the phononic crystal direction x , the mode function can be approximated as $\vec{u}_{n,k}(\vec{r}) \sim \vec{e}_x \cos(\omega_{n,k}x/v_l)$, leading to $|\varsigma_{n,k}(\vec{r})| = 1$.

Band-gap interactions between single SiV centers and acoustic modes

As discussed in the main text, we consider the case where the transition frequency of the defect center is tuned close to the band edge. Then the spin is dominantly coupled to the modes near the band edge wavevector $k_0 = \pi/a$ due to the van Hove singularity in the density of states, i.e., $\frac{\partial k}{\partial \omega_k}|_{k_0} \rightarrow \infty$. In this case, the dispersion relation can be approximated to be quadratic $\omega_k \simeq \omega_{\text{BE}} - \alpha a^2(k - k_0)^2$, with α a parameter characterizing the band curvature. In the presence of a static magnetic field $\vec{B} = B_0 \vec{e}_z$ and a microwave driving field of frequency ω_0 and Rabi-frequency Ω along \vec{e}_x , we can implement a Raman transition between the states $|g\rangle$ and $|e\rangle$ via the excited state $|f\rangle$ through coupling the SiV center to the mechanical modes. In the interaction picture, the full Hamiltonian is given by

$$\hat{\mathcal{H}} = \sum_k \hbar g_k \hat{a}_k e^{ikx_0} (\hat{\sigma}_{fg} + \hat{\sigma}_{de}) e^{i\delta_{\text{BE}}t} + \hbar\Omega \hat{\sigma}_f e^{i\delta t} + \text{H.c.} \quad (\text{S26})$$

In the dispersive limit, i.e., $\delta_{\text{BE}}, \delta \gg g_k, \Omega$, and after adiabatic elimination of the excited states $|f\rangle$ and $|d\rangle$, we obtain the effective interaction Hamiltonian

$$\hat{\mathcal{H}} = \sum_k \hbar g_{\text{eff}} (\hat{a}_k \hat{\sigma}_{eg} e^{ikx_0} e^{i\Delta_{\text{BE}}t} + \text{H.c.}), \quad (\text{S27})$$

with $\Delta_{\text{BE}} = \Delta - \delta - \omega_{\text{BE}}$. In the Schrödinger picture, we have

$$\hat{\mathcal{H}} = \sum_k \hbar\omega_k \hat{a}_k^\dagger \hat{a}_k + \hbar\omega_s \hat{\sigma}_{ee} + \sum_k \hbar g_{\text{eff}} (\hat{a}_k^\dagger \hat{\sigma}_{ge} e^{-ikx_0} + \hat{a}_k \hat{\sigma}_{eg} e^{ikx_0}). \quad (\text{S28})$$

For a single excitation in the system, there exists a bound state

$$|\varphi_b\rangle = \cos\theta|0\rangle|e\rangle + \sin\theta|1\rangle|g\rangle \quad (\text{S29})$$

within the bandgap with the eigenenergy $\hbar\Omega_b$. Here $|0\rangle$ is the vacuum state for the phonon modes, and $|1\rangle = \int dk c_k \hat{a}_k^\dagger |0\rangle$ is a single phonon excitation of the modes in the band. The bound state and the corresponding eigenenergy are determined by the eigenvalue equation

$$\hat{\mathcal{H}}|\varphi_b\rangle = \hbar\Omega_b|\varphi_b\rangle. \quad (\text{S30})$$

From this equation we have

$$\cos\theta(\Omega_b - \omega_s) = \sin\theta \sum_k g_{\text{eff}} c_k e^{ikx_0} \quad (\text{S31})$$

$$c_k \sin\theta(\Omega_b - \omega_k) = g_{\text{eff}} \cos\theta e^{-ikx_0}. \quad (\text{S32})$$

Solving these equations yields

$$c_k = \frac{g_{\text{eff}} e^{-ikx_0}}{\tan\theta(\Omega_b - \omega_k)} \quad (\text{S33})$$

$$\Omega_b - \omega_s = \sum_k \frac{g_{\text{eff}}^2}{\Omega_b - \omega_k} \quad (\text{S34})$$

$$\tan^2\theta = \sum_k \frac{g_{\text{eff}}^2}{(\Omega_b - \omega_k)^2}. \quad (\text{S35})$$

When we take $\omega_k \simeq \omega_{\text{BE}} - \alpha a^2(k - k_0)^2$, and change from a discrete modes to a continuous distribution, we can obtain

$$\Omega_b - \omega_s = \frac{\pi g_{\text{eff}}^2}{\sqrt{\alpha(\Omega_b - \omega_{\text{BE}})}} \quad (\text{S36})$$

$$\tan^2(\theta) = \frac{\omega_s - \Omega_b}{2(\omega_{\text{BE}} - \Omega_b)} \quad (\text{S37})$$

$$c_k = \frac{g_{\text{eff}} e^{-ikx_0}}{\tan\theta(\Omega_b - \omega_k)}. \quad (\text{S38})$$

In real space, the phononic part of the bound state is exponentially localized around the spin with spatial mode envelope

$$\mathcal{E}(x) = \int dk c_k Q_k(x) = \sqrt{\frac{2\pi}{L_c}} e^{-|x-x_0|/L_c} Q_{k_0}. \quad (\text{S39})$$

Band gap engineered spin-spin interactions between distant SiV centers

As discussed in the main text, the band-gap interaction allows us to use the phononic crystal modes as a quantum bus to perform more complex tasks. Analogous to the spin-exchange interaction in cavity QED, two defect centers that are separated by a distance on the order of the length L_c can exchange a phonon excitation via the induced acoustic cavity mode. We consider two separated SiV centers coupled to the same phononic crystal modes near the band edge, through Raman transitions between the states $|g\rangle$ and $|e\rangle$. In the interaction picture, we can obtain the interaction between the defect centers and phononic crystal modes

$$\hat{H} = \sum_{j=1,2} \sum_k \hbar g_{\text{eff}}^j (\hat{a}_k^\dagger \hat{\sigma}_{ge}^j e^{-i\delta_k t - ikx_j} + \hat{a}_k \hat{\sigma}_{eg}^j e^{i\delta_k t + ikx_j}) \quad (\text{S40})$$

with $\delta_k = \omega_s - \omega_k$. In the dispersive regime $\delta_k \gg g_{\text{eff}}^j$, this will lead to an effective spin-spin interaction via the exchange of virtual phonons. With the phononic modes eliminated, the interaction is described by the effective Hamiltonian

$$\hat{H} = \hbar \hat{\sigma}_{eg}^1 \hat{\sigma}_{ge}^2 g_{\text{eff}}^2 \int dk \frac{e^{ik(x_1-x_2)}}{\omega_s - \omega_k} + \text{H.c.} \quad (\text{S41})$$

We can integrate over the phononic modes and apply the same approximation near the band edge as used to derive the bound state. To first order in Δ_{BE}^{-1} , the interaction becomes

$$\hat{\mathcal{H}}_{s-s} = \frac{\hbar g_c^2}{2\Delta_{\text{BE}}} e^{-|x_1-x_2|/L_c} \hat{\sigma}_{eg}^1 \hat{\sigma}_{ge}^2 + \text{H.c.} \quad (\text{S42})$$

We can generalize the above results to the case where an array of distant defect centers are coupled with the band-gap mediated interaction. This opens another exciting perspective for quantum simulation, with spin-spin Hamiltonians for quantum magnetism of the general form

$$\hat{H}_{\text{spin}} = \sum_{\alpha=x,y,z} \sum_{i,j} J_{i,j}^{\alpha} \hat{\sigma}_{\alpha}^i \hat{\sigma}_{\alpha}^j, \quad (\text{S43})$$

where $\hat{\sigma}_{\alpha}^i$ are Pauli operators and $J_{i,j}^{\alpha}$ are the spin-spin interaction energies in the α direction for sites i and j . Here, the range of interactions has an exponentially decaying envelope, i.e., $J_{i,j}^{\alpha} \sim e^{-|x_i-x_j|/L_c}$, and is restricted to nearest neighbours.

[S1] L. D. Landau and E. M. Lifshitz, *Theory of Elasticity* (Butterworth-Heinemann, Oxford, 1986).

[S2] COMSOL Multiphysics 3.5, <http://www.comsol.com/>

[S3] M. Aspelmeyer, T. J. Kippenberg, and F. Marquardt, *Cavity Optomechanics* (Springer, Berlin, 2014).

[S4] K. V. Kepesidis, M.-A. Lemonde, A. Norambuena, J. R. Maze, and P. Rabl, Cooling phonons with phonons: Acoustic reservoir engineering with silicon-vacancy centers in diamond, *Phys. Rev. B* 94, 214115 (2016).